Journal of Chemistry Studies
DOI: 10.32996/jcs
Journal Homepage: www.al-kindipublisher.com/index.php/jcs

JCS
AL-KINDI CENTER FOR RESEARCH AND DEVELOPMENT

| RESEARCH ARTICLE

A Simple Two-Dimensional Convective-Diffusive Based Modelling Study of a Biosensor for Glucose Detection

Victus Kordorwu[1], Isaac D. Tegladza[2] ✉ and Emmanuel Okoampah[3]

[1]*Department of Chemical Engineering, Northeastern University, 360 Huntington Ave, Boston MA 02115, United States.*
[2]*College of Chemical Engineering, Nanjing Tech University, Nanjing Jiangsu 211816, China.*
[3]*Department of Biochemistry, Faculty of Bioscience, University for Development Studies, Tamale, Ghana*

Corresponding Author: Isaac D. Tegladza, **E-mail**: 2393902638@qq.com

| ABSTRACT

Over the past decade, novel technologies for biomolecular detection of target molecules of interest have been reported. The chemical reactions that govern the kinetics of the transport of target molecules to the sensor are also of significant importance. Here we analyze how the diffusion, convection, and reaction kinetics can drive the experimental design of a simple glucose biosensor. In this work, a physically intuitive and practical understanding of analyte transport is presented by modelling and simulating a two-dimensional convective-diffusive transport phenomenon in COMSOL Multiphysics to understand the mechanism of surface capture dynamics of a biosensor under the assumption of perfect binding kinetics. The target molecule of interest is glucose. In the model, 1 mol/m^3 of the glucose solution is introduced at the inlet at 1 mm/s, and the process is simulated as a stationary study. It was found that by decreasing the flow rate, a threshold exists where the detection of target molecules by the sensor is solely controlled by diffusion. Comparison of convective and diffusive fluxes of the system as well as the concentration distribution reveal that a decrease in flow rate increases diffusive transport, thus increasing the fraction of target molecules that are captured by the sensor.

| KEYWORDS

Non-invasive Glucose Detection; Biosensors; Reaction Kinetics; COMSOL Modeling; Microfluidic Devices

| ARTICLE INFORMATION

ACCEPTED: 25 July 2022 **PUBLISHED:** 30 July 2022 **DOI:** 10.32996/jcs.2022.1.2.1

1. Introduction

Biosensors are useful for a wide range of industries and application areas, such as food manufacturing and medical devices. A biosensor is an electronic device that has a biological probe and a transducer that is connected to a monitor. The demand for a wide variety of applications for a biosensor in industrial, environmental, and biomedical diagnostics is dramatically increasing [Zhu, 2013; Wen, 2009; Zhu, 2010; Squires, 2008; Wang, 2020]. Biomedical applications, such as non-invasive blood glucose detection, demand plenty of research activities. Glucose oxide (GOx)-based enzyme sensors have been applied for the diagnosis and monitoring of blood glucose levels due to their ability to quickly and precisely identify glucose target molecules [Zhu, 2013; Wen, 2009; Zhu, 2010]. Although both chemical kinetics and the transport process involved in the detection of glucose to the sensor are equally vital, the relationship between these processes has been minimally explored [Squires et al., 2008].

As such, this simple modelling study is designed to investigate the effects of convection, diffusion, and reaction kinetics in a two-dimensional diffusive-conversive driven model of glucose molecule transport in a biosensor. In this model, a channel of height H and width W has the target solution flowing through at a volumetric flow rate, Q (containing a sensor of width Ws and length L in the flow direction). The following assumptions are adopted; (i) the sensor is functionalized with (per unit area of) receptors, (ii) the solution contains target molecules (with concentration c_0 and diffusivity D), and (iii) target molecules in solution only bind receptors

on the sensor and do not bind to the sensor substrate and (iv) the nature of binding is perfect [Squires et al., 2008]. The modelling and finite element computations are carried out with COMSOL Multiphysics [COMSOL, 2018].

2. COMSOL Modelling and Simulation

Modeling and simulation of convective-diffusive transport of species depend on geometry and feature sizes, feature mesh, and the chosen materials. A rectangular geometry of dimensions 6.0 x 1.0 mm is chosen to mimic a microfluidic device. The model is categorized into three sections, the inflow region, the sensor region, and the outflow region. Water is used as the medium of transport. **Fig. 1** shows the model of the system. Laminar flow and transport of dilute species modes were used to simulate flow and mass transport, respectively, in a stationary study. In this process, a solution containing 1.0 mol/m^3 of the target molecule is introduced at 0.001 m/s at the inlet. A fast irreversible surface reaction is modelled on the surface of the sensor with a negative stoichiometric coefficient to denote the binding or consumption of target molecules by diffusion across the surface. It is assumed that there is a perfect binding of the sensor to the target molecules. The diffusivity of the specie was set at 10^{-9} m^2/s. The mesh size for the whole structure was defined and optimized using finer mode in the COMSOL.

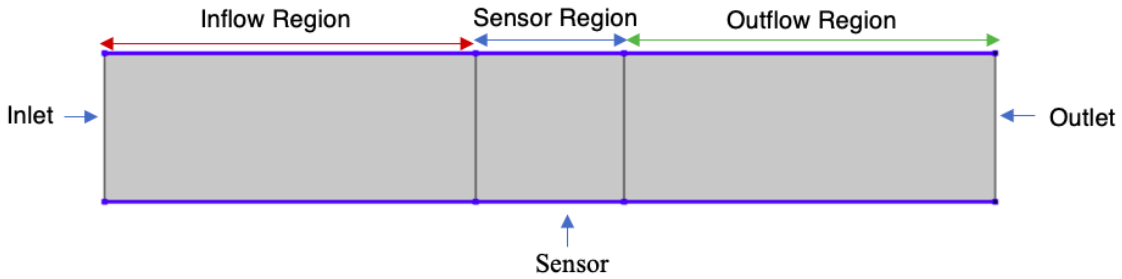

Fig. 1: The schematic of the model.

2.1 Theory

The process is characterized by the diffusion of *n* species and the simultaneous consumption of their molar concentration. The operation of the sensor can be described as a diffusion-reaction problem. Under the assumption of isothermal conditions and uncoupled diffusion, the diffusion-reaction process for each species can be expressed by [Diamond, 1998; Farronato, 2022; Jain, 2021]:

$$\frac{\partial c_i}{\partial t} + \nabla \cdot \{D_i \nabla c_i\} = \sum_{j=1\, i\neq 1}^{n} k_{ij}\, c_i c_j \qquad (1)$$

Where D_i is diffusion coefficient (m^2/s) and k_{ij} generates coupling between the species concentrations: each component governs the rate of the reaction between species i and j (the case $j = i$ is not considered).

The transport of the target molecule, glucose, is expressed by $n \cdot D_i \nabla c_i = 0$ with $c_o = 1$ mol/m^3 where c_0 is initial concentration (mol/m^3). The stationary study for the flow is expressed by $-n \cdot J_i = 0$, $c = 0$, and $u = 0$, denoting a no slip boundary condition at the wall. The inlet flow velocity, u_0, is 0.001m/s. The irreversible fast surface reaction occurring at the surface of the sensor is expressed by;

$$n \cdot J_i = \nu_i r \qquad (2)$$

$$r: c_{lim} = 0 \qquad (3)$$

$$\sum_{i,\nu_i<0} \nu_i S_i \rightarrow \sum_{i,\nu_i>0} \nu_i S_i \qquad (4)$$

Where c_{lim} and ν_i denote rate limiting species concentration and stoichiometric coefficients, respectively. The stoichiometric coefficient was set to -1 to denote the consumption of species.

The flow of water in the channel is described Navier-Stokes equation, given by

$$\rho \frac{DU}{Dt} = -\nabla \mathrm{P} + \rho \mathrm{g} + \eta \nabla^2 U \qquad (5)$$

Where ρ, U, P, g, and η are density, velocity field, pressure, gravity, and viscosity, respectively. To achieve the field velocity of the water, Navier-stocks equations must be simultaneously solved with the continuity equation given by;

$$\frac{\partial \rho}{\partial t} + \nabla(\rho U) = 0 \qquad (6)$$

Since water is incompressible, ρ becomes constant; therefore, the equation is reduced to $\nabla U = 0$.

3. Simulation Results and Discussions

The velocity distribution of the system, as shown in **Fig. 2,** is a laminar flow profile with the slowest flow occurring at the walls and a parabolic distribution of flow rates evolving laterally across the channel. 1 mm/s of inflow velocity of the sample solution containing the target molecule was applied along the entire channel width at the inflow region. The flow at the inlet region quickly transitions into a fully developed flow at 0.5 mm from the inlet and attains a maximum velocity of 1.4 mm/s.

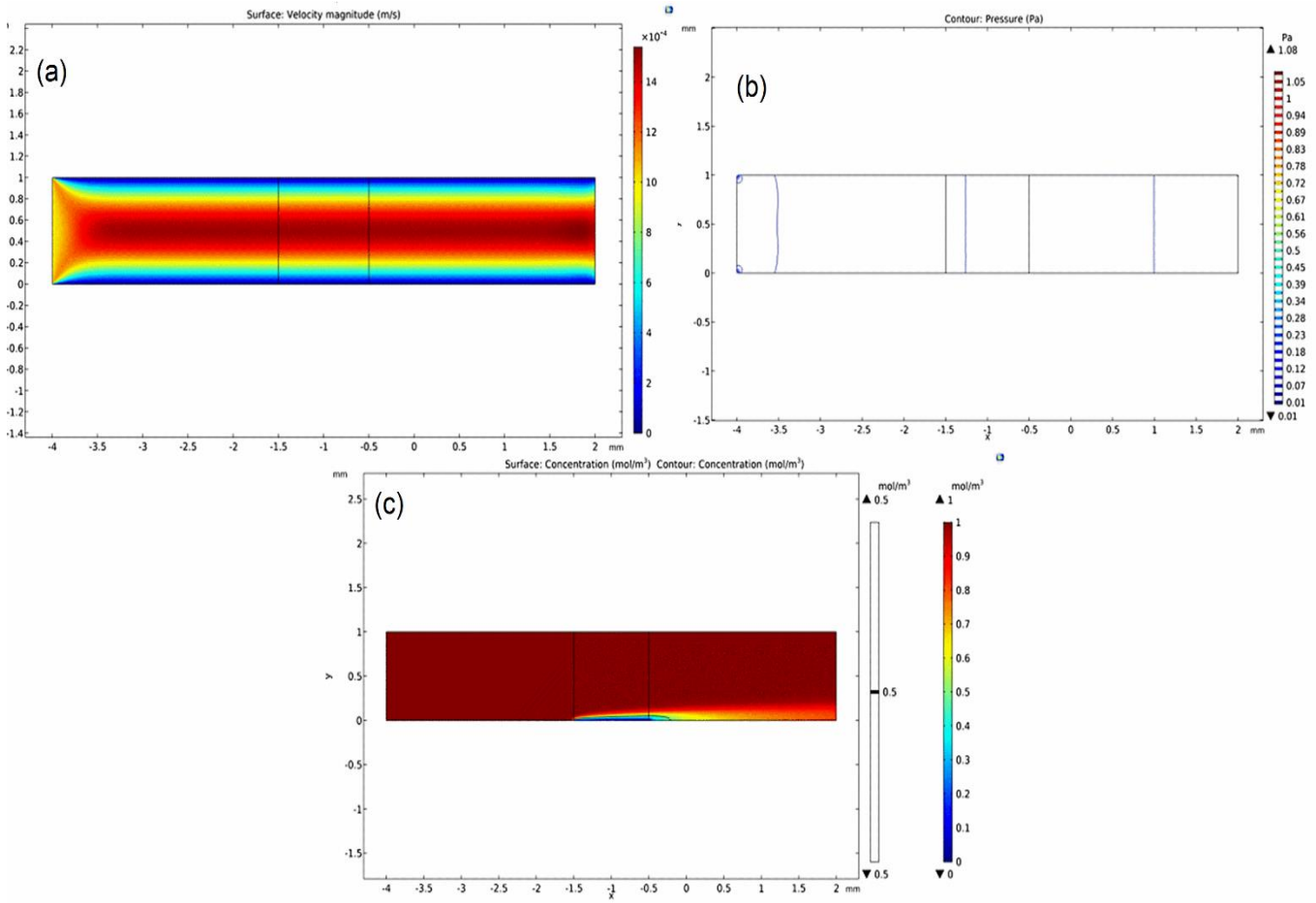

Fig. 2: Surface velocity magnitude (a), contour pressure (b), and surface and contour concentration profiles (c) of the system.

A blue planar depletion zone develops at the onset of the operation of the diffusion-based sensor. The blue planar depletion zone close to the surface of the sensor signifies diffusion of the target molecule into the sensor as diffusion provides fresh target molecules to the sensor over time. The flow induces an asymmetry from left to right as the fresh solution of unbound target molecules flows in from the left as some of it is depleted due to diffusion. The remaining molecules are transported laterally by diffusion and captured by the sensor, while the right channel has some of its target molecules depleted. The black line represents a mid-point concentration. The fluid below and inside the 0.5 mark (black line) is depleted of at least half of its target solute content, whereas the region above it contains more than half of the solute content.

3.1 Effect of Flow Rate on Concentration

The simulation results showing different flowrates by decreasing the flow velocity by various order of magnitudes are shown in **Fig. 3**. At 10^{-4} m/s, the depletion zone thickness increases, and as the flow is decreased further (Fig 3a), more of the larger fraction of the target molecule flowing into the system is captured on to the sensor. At 10^{-5} m/s, the depletion region evolves from a thin plane into a radial shape (Fig 3b). There is increased depletion downstream in the outflow region because that is the direction of fluid flow. Interestingly, the depletion area in the inflow region grows upstream to the left. This implies that the system is reaching a slow enough flow that some target molecules diffuse faster than they are flowing.

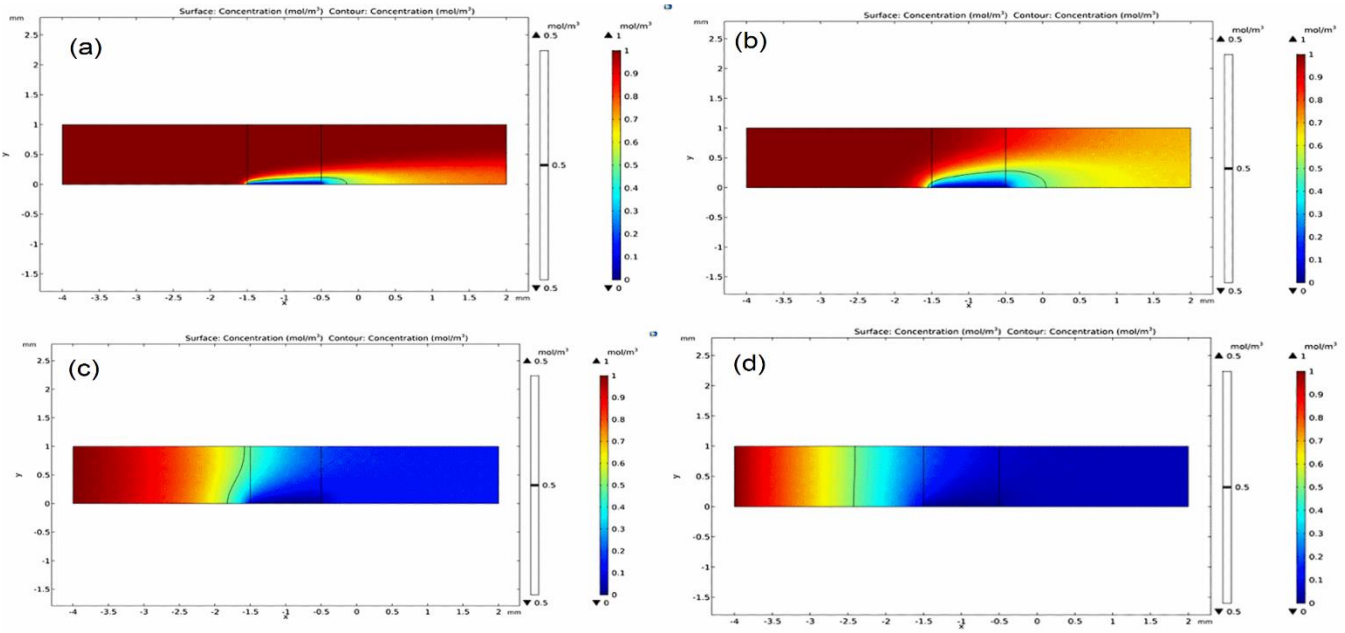

Fig. 3: Concentration profiles at various flow velocities, (a) u = 10^{-4} m/s, (b) u = 10^{-5} m/s, (c) u = 10^{-6} m/s, (d) u = 10^{-7} m/s

At 10^{-6} m/s, a major transition occurs as the 50 % mark (black line, Fig. 3c) quickly reaches the top of the channel and approaches linearity. In this regime, the depletion zone grows linearly in both left and right directions compared to the planar and radial regime, where it grew vertically. This flow velocity represents a threshold at which the transport of solute target molecules to the surface of the sensor is controlled by diffusion. At an even slower velocity, 10^{-7} m/s (Fig 3d), the depletion zone becomes linear, and the sensor consumes all the target molecules by random diffusion. It is thus demonstrated that there exists a critical flow rate or velocity at which not only the region of the channel content gets depleted, but the entire channel content gets depleted as well.

3.2 Evolution of Concentration with Height of Channel

Fig. 4(a-d) illustrates the variation of concentration with the height of the channels. The concentration profile of the target solute molecule in the inflow region (red line) from wall to wall is linear and decreases in magnitude with a decrease in velocity due to increased diffusion at low velocities.

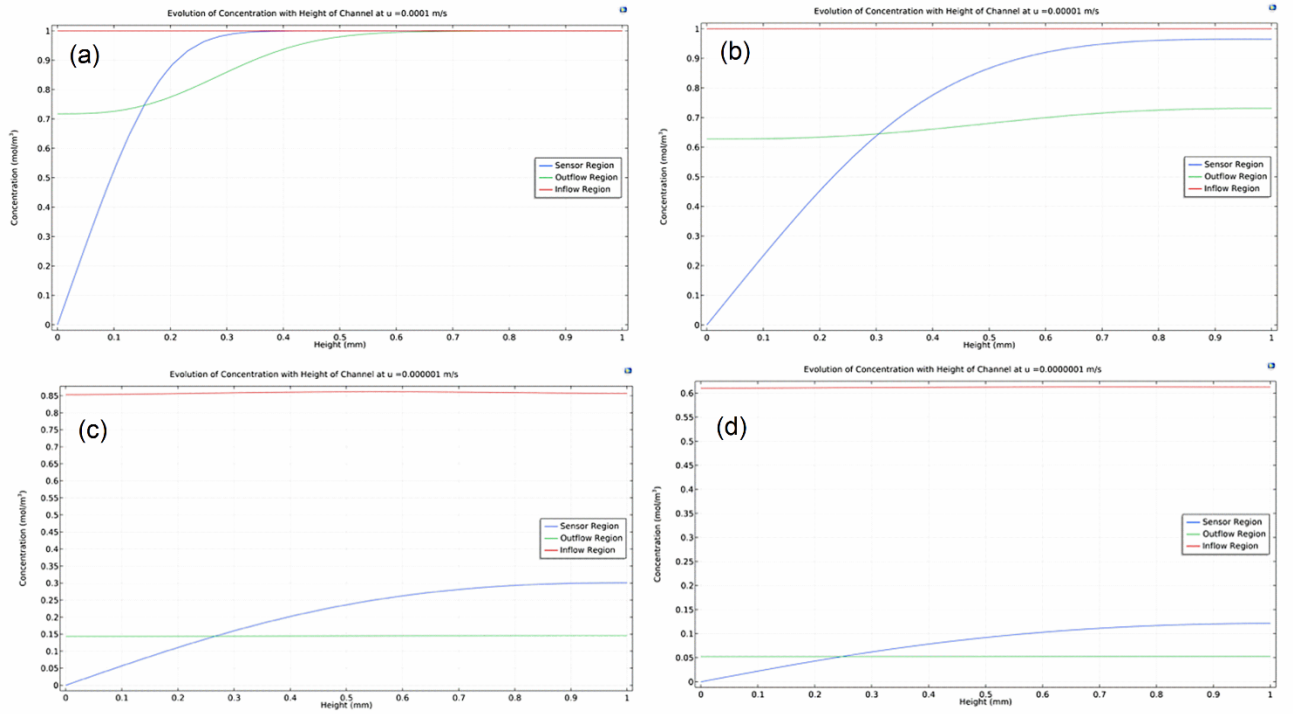

Fig. 4: Vertical variation of concentration in the channels at (a) u = 10^{-4} m/s, (b) u = 10^{-5} m/s, (c) u = 10^{-6} m/s, (d) u = 10^{-7} m/s.

In the sensor region (blue line), the concentration above the 0.5 mark line decreases non-linearly and rapidly with a decrease in velocity due to increased depletion of target molecules due to diffusion. In the outflow region (green line), convective transport is initially high, and depletion of target molecules is low; thus, a high amount of unbound target molecules exist. A decrease in velocity increases diffusive transport of the molecules, and increased diffusion decreases the concentration of unbound molecules.

3.3 Evolution of Concentration with Length of Channel

Figs. 5-7 (a-c) shows the entire distribution of concentration across the entire length of the sensor (Fig. 5 center, Fig. 6 top, and Fig. 7 bottom of the channel, respectively). From **Fig. 5**, the distribution of concentration reflects the dominance of diffusive transport at low velocities at the center of the channels with a decrease in velocity. The species concentration at the inflow region drastically transitions from a constant linear profile with no gradient into one with a steep gradient when the velocity decreases to 10^{-7} m/s.

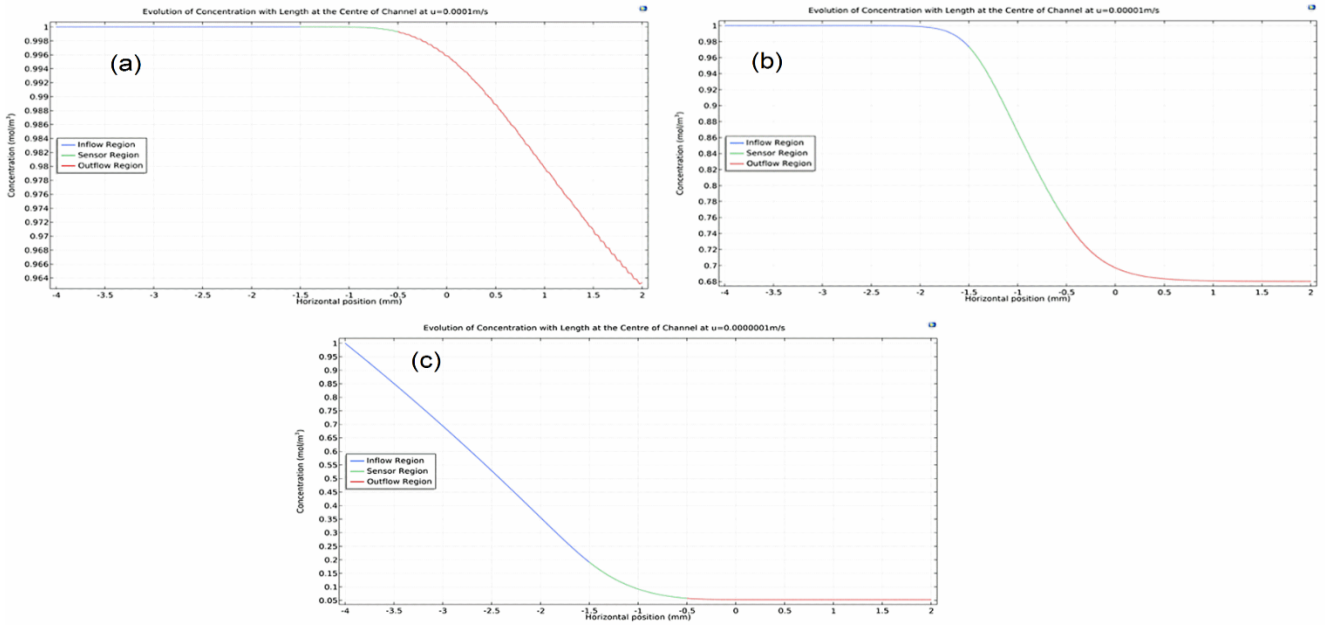

Fig. 5: Horizontal variation of concentration at the center of the channels (a) $u = 10^{-4}$ m/s, (b) $u = 10^{-5}$ m/s, (c) $u = 10^{-7}$ m/s.

Diffusion in the sensor region increases as the area of target molecules consumption increases resulting in a decrease in concentration. This effect extends to the outflow region, where the concentration decreases as well.

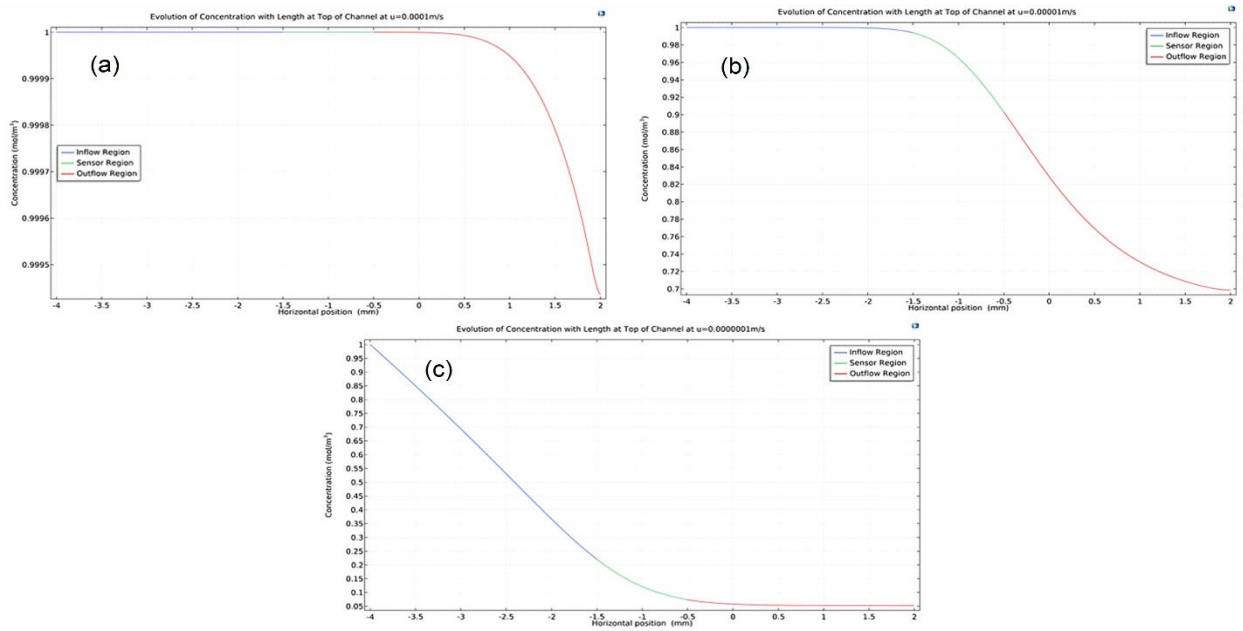

Fig. 6: Horizontal variation of concentration at the top of the channels (a) $u = 10^{-4}$ m/s, (b) $u = 10^{-5}$ m/s, (c) $u = 10^{-7}$ m/s.

The distribution profile of concentration at the top of the channel (**Fig. 6**) follows a similar trend as the distribution profile at the center of the channels for the same reason. At the bottom of the channels shown in **Fig. 7,** however, the concentration of the target molecules in the sensor region remains low and constant with a decrease in velocity.

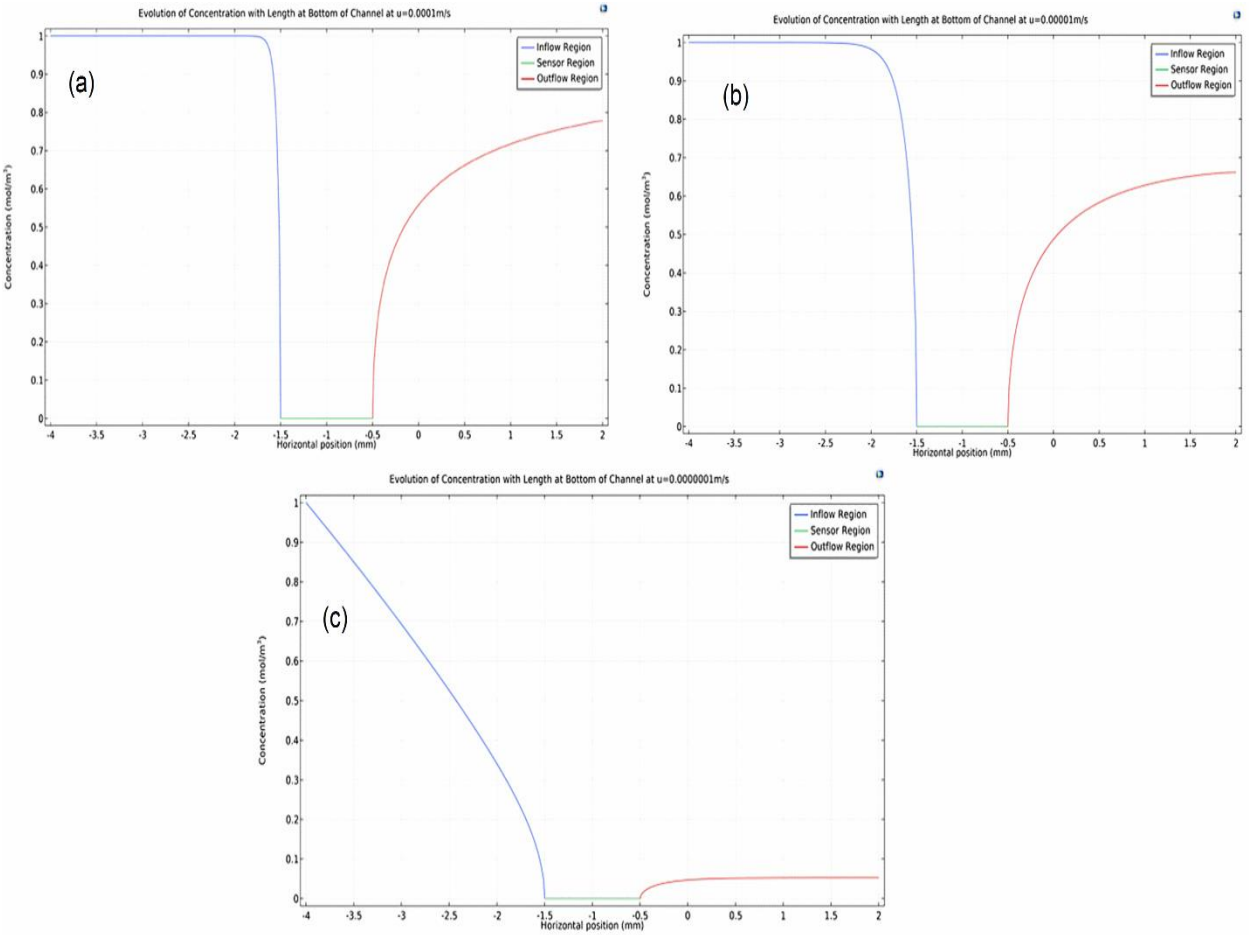

Fig. 7: Horizontal variation of concentration at the bottom of the channels, (a) $u = 10^{-4}$ m/s, (b) $u = 10^{-5}$ m/s, (c) $u = 10^{-7}$ m/s.

The concentration in the inflow and outflow regions at the bottom of the channels, however, transitions from a steep decline and a parabolic distribution to a gentle slope and a linear distribution, respectively, with decreased velocity due to the transition of the shape of the 0.5 mark from radial to linear in both regions.

3.4 Evolution of Diffusive and Convective Fluxes

The evolution of convective and diffusive fluxes for flow velocities 10^{-3}, $10^{-5,}$ and 10^{-7} m/s is shown in **Fig. 8**. The convective flux at the inflow region follows the parabolic profile of a fully developed laminar flow. The flux is highest at the center of the channel and zero at the walls. A decrease in velocity of the flow skews the parabolic distribution of the inflow convective flux to the right due to increased diffusion. At lower velocities, the transport of solute molecules is predominantly controlled by diffusion, and the diffusive area increases. The inflow diffusive flux is low and decreases in slope due to lower diffusive activity near the wall.

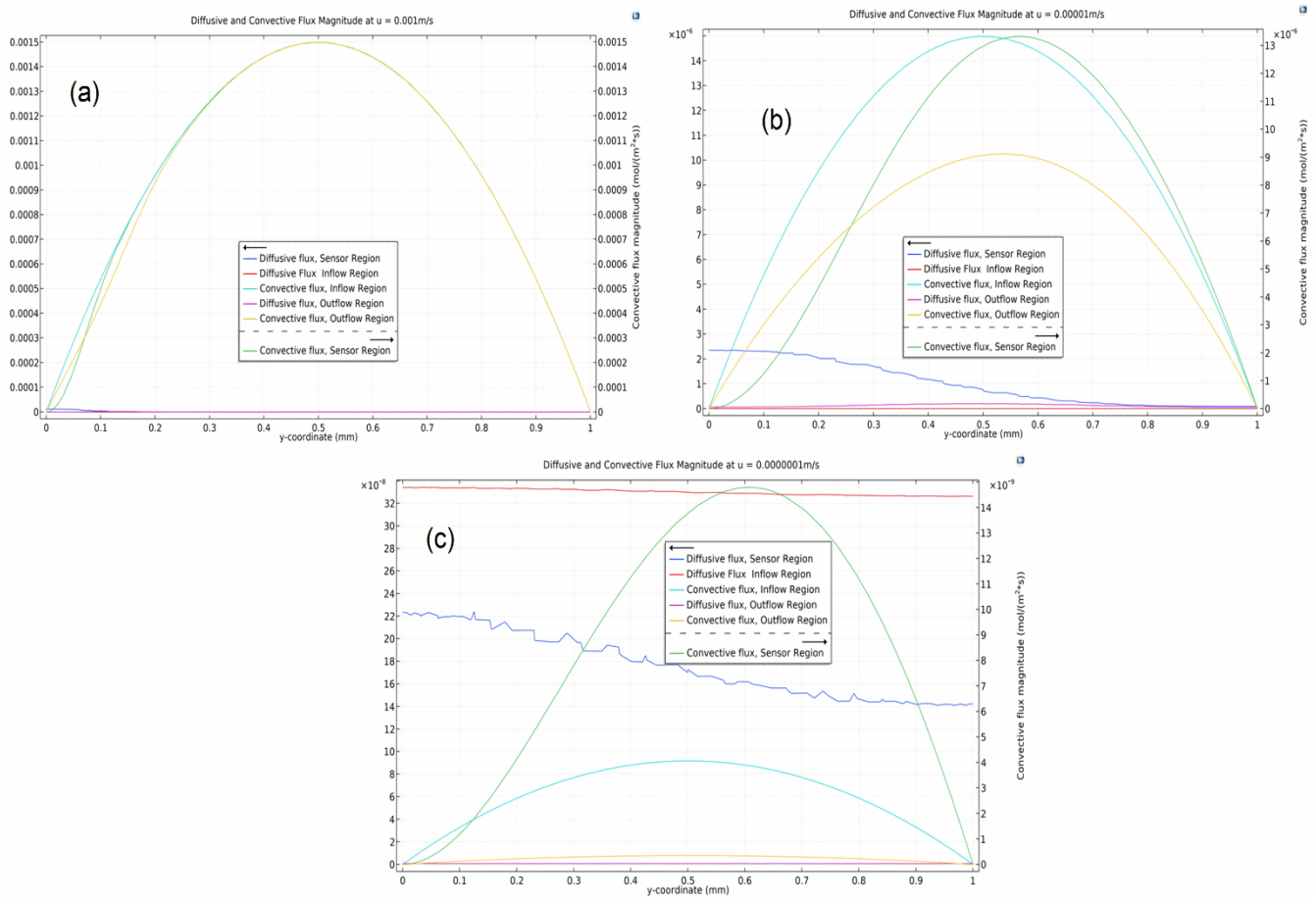

Fig. 8: Evolution of convective and diffusive fluxes. The y -axis on the left represents diffusive flux, (a) $u = 10^{-3}$ m/s, (b) $u = 10^{-5}$ m/s, (c) $u = 10^{-7}$ m/s.

The diffusive flux in the sensor region is higher near the surface of the sensor due to increased diffusive transport of target molecules into the sensor and decreases towards the wall because of convection. However, the decrease in diffusive flux towards the wall is gentle at the lowest velocity due to decreased convective transport. In the outflow region, the concentration remains low while the parabolic distribution of the convective flux decreases with a decrease in flow velocity due to low convective transport and the extension of the diffusion region when the process is dominated by diffusion.

4. Conclusions

A two-dimensional convective diffusive based modelling of a biosensor is conducted using COMSOL Multiphysics simulation software. The model is an aggregation of microfluidic chips of rectangular geometry categorized into three sections, the inflow, sensor, and outflow regions. In the model, a 1 mol/m^3 of the sample solution is introduced at the inlet at 1 mm/s, and the process is simulated as a stationary study. It was found that by decreasing the flow rate, a threshold exists where the detection of target molecules by the sensor is solely controlled by diffusion. Comparison of convective and diffusive fluxes of the system as well as the concentration distribution reveal that a decrease in flow rate increases diffusive transport, thus increasing the fraction of target molecules that are captured by the sensor.

Funding: This research received no external funding.
Conflicts of Interest: The author declares no conflict of interest
Acknowledgment: The views expressed in this paper are those of the authors and do not represent the views of any affiliated institution.

References

[1] COMSOL Inc. (2018). COMSOL Multiphysics. R Reference Manual. 5.4.
[2] Diamond D. (1998). *Principles of Chemical and Biological Sensors*. New York: Wiley.
[3] Farronato, G., Cefis, N. and Fedele, R. (2022). Numerical modelling in Comsol Multiphysics of a multispecies diffusion-reaction problem for concrete elements. In AIP Conference Proceedings 2425(1):300003-5.
[4] Jain, A., Gencturk, B. (2021). Multiphysics and Multiscale Modeling of Coupled Transport of Chloride Ions in Concrete. Materials, 14, 885.
[5] Squires T.M, Messinger R.J and Manalis S.R. (2008). Making it stick: convection, reaction, and diffusion in surface-based biosensors, *Nature Biotech., 26*(4):417-426.
[6] Wang X.D and Wolfbeis O.S. (2020). Fiber-optic chemical sensors and biosensors. Anal. Chem. 92:397−430.
[7] Wen Z, Ci S, and Li J. (2009). Pt nanoparticles inserting in carbon nanotube arrays: nanocomposites for glucose biosensors. J Phys Chem C, 113:13482–13487.
[8] Zhu Z.G, Garcia-Gancedo L, Chen C, Zhu X.R, Xie H.Q, Flewitt A.J, and Milne W.I. (2013). Enzyme-free glucose biosensor based on low-density CNT forest grown directly on a Si/SiO2 substrate. Sens Act B-Chem. 178:586–592.
[9] Zhu Z, Song W, Burugapalli K, Moussy F, Li Y-L, and Zhong X-H. (2010). Nano-yarn carbon nanotube fiber-based enzymatic glucose biosensor. Nanotechnology. 21:165501